AIP Applied Physics Letters

Gas loading of graphene-quartz surface acoustic wave devices

E. F. Whitehead, E. M. Chick, L. Bandhu, L. M. Lawton, and G. R. Nash

Citation: Appl. Phys. Lett. **103**, 063110 (2013); doi: 10.1063/1.4818465
View online: http://dx.doi.org/10.1063/1.4818465
View Table of Contents: http://apl.aip.org/resource/1/APPLAB/v103/i6
Published by the AIP Publishing LLC.

Gas loading of graphene-quartz surface acoustic wave devices

E. F. Whitehead, E. M. Chick, L. Bandhu, L. M. Lawton, and G. R. Nash[a)]
College of Engineering, Mathematics and Physical Sciences, University of Exeter, Exeter EX4 4QF, United Kingdom

(Received 14 June 2013; accepted 28 July 2013; published online 9 August 2013)

Graphene was transferred to the propagation path of quartz surface acoustic wave devices and the attenuation due to gas loading of air and argon measured at 70 MHz and 210 MHz and compared to devices with no graphene. Under argon loading, there was no significant difference between the graphene and non-graphene device and the values of measured attenuation agree well with those calculated theoretically. Under air loading, at 210 MHz, there was a significant difference between the non-graphene and graphene devices, with the average value of attenuation obtained with the graphene devices being approximately twice that obtained from the bare quartz devices.
 [http://dx.doi.org/10.1063/1.4818465]

Although graphene's large surface area and unique properties, including its sensitivity to single absorbed molecules,[1] means that it naturally lends itself to potential integration with surface acoustic wave (SAW) devices, relatively little work has so far been reported. SAWs propagate along the surface of a solid, with the majority of the energy of the wave confined within one wavelength of the surface. SAW based devices are widely used, for example in mobile phones and televisions, and in such a device a radio frequency signal is applied to an interdigital transducer, on a piezoelectric substrate, to launch a SAW pulse. An identical transducer can be used to detect the SAW at the other side of the device. As the attenuation and velocity of the SAW can be dramatically affected by its interaction with the surface of the device, SAWs are also widely used in sensing applications due to the ability to make devices with relatively large sensing areas.[2] Thalmeier *et al.*[3] and Zhang *et al.*[4] have both made theoretical studies of the change in SAW propagation, on a piezoelectric substrate, due to the interaction with charge carriers in graphene. Acousto-charge transport, which exploits this piezoelectric interaction, has been reported from large graphene sheets transferred onto lithium niobate substrates,[5] and very recently in monolayer graphene on SiC.[6] Arrat *et al.*[7] deposited graphene like nano-sheets, prepared by the reduction of graphene oxide, onto $LiTaO_3$ SAW devices and used these to sense hydrogen and carbon monoxide. The effects of moisture adsorbed on 200 nm multilayer graphene sheets and the resulting SAW attenuation was investigated experimentally by Ciplys *et al.*[8] They report that ambient air humidity produced an exponential increase in attenuation as a function of frequency, but from these measurements alone it is difficult to determine the mechanism of this attenuation. In this paper, we investigate the effects of argon and air loading on quartz SAW devices, which have the advantage of greater temperature stability (negligible temperature coefficient of delay) compared to other substrates, with and without graphene in the acoustic path.

Commercially available CVD graphene grown on copper was transferred onto ST-cut quartz SAW bandpass filters, with a 1 dB bandwidth of 1.3 MHz at 70 MHz, using the PMMA transfer technique.[9] A 100 nm thick layer of PMMA was drop coated on the graphene, and baked at 180 °C for 10 min. The copper was then etched away using 0.3 M $FeCl_3$ solution, leaving a thin sheet of PMMA/graphene floating on the surface. This flake was rinsed in deionized water 8–10 times to remove any residual etchant and transferred to the quartz substrate. The sample was allowed to dry at room temperature to allow proper adherence of the graphene to the quartz. Finally the PMMA was removed in boiling acetone (80 °C for 30 min) leaving a graphene sheet of approximately 3 mm × 3 mm on the quartz surface between the interdigital transducers.

Characterization of the graphene was undertaken using Raman spectroscopy, with a Renishaw 100 mW CW 532 nm laser. Raman spectra were measured at nine points randomly distributed across the graphene sheet and the average of these spectra, together with the average obtained from five points measured in the bare quartz, is plotted in Figure 1. Note that the bare quartz spectrum has been subtracted from the graphene spectrum. The 2D and G peak were obtained at 2885 cm^{-1} and 1590 cm^{-1}, respectively, and the 2D/G peak ratio was measured to be 1.83 which is characteristic of graphene.[10] A relatively small D peak at 1346 cm^{-1}, which could be attributed to the defects caused by the unintentional doping and wrinkles formed during the transfer process, suggests that the overall quality of the transferred graphene is high. Two metal contacts, 3.5 mm by 40μm (separation = 1.5 mm), were then defined using e-beam lithography to sit on top of the graphene and in the acoustic path as shown schematically in Figure 2. Metallization was done by thermal evaporation of 5 nm Cr and 50 nm Au. The samples were then mounted on a printed circuit board (PCB) using a conductive silver epoxy and measurements were undertaken with the PCB mounted in a vacuum chamber at room temperature. Four devices were investigated: two with graphene and two without.

Measurements were performed by exciting 0.5μs long SAW pulses, with a repetition frequency of 200 kHz, at the transmitter and receiving the time-delayed signal at the opposing transducer. The amplitude of the received SAW was measured using a LeCroyWaveRunner 204Xi-A digital oscilloscope. The acoustic path length of the devices was 10.8 mm

a)Author to whom correspondence should be addressed. Electronic mail: g.r.nash@exeter.ac.uk

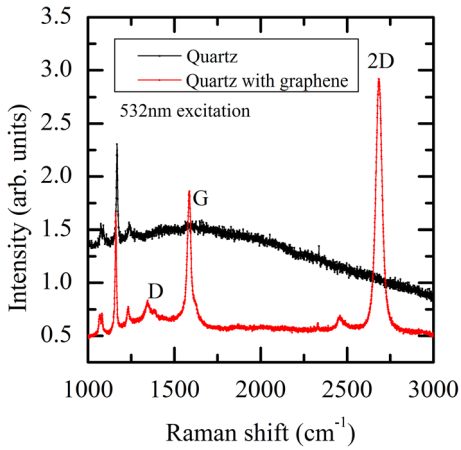

FIG. 1. Raman spectrum of the graphene layer on the quartz surface between DC probe contacts showing the characteristic D, G, and 2D peaks. The 2D/G peak ratio was measured to be 1.83, which is characteristic of single layer graphene.

and the transducers had resonances at 70 MHz and 210 MHz. Note that the large bandwidth of the devices means that changes in the velocity of the SAW caused by gas loading will not manifest themselves as a change in SAW amplitude.

To obtain the attenuation due to air and argon loading the SAW amplitude was measured with the chamber either evacuated or filled with gas. For the first stage, the device rested in the sealed chamber filled with gas at atmospheric pressure for 10 min and the SAW amplitude was measured. The SAW amplitude was then measured every second as the chamber was evacuated. In all of the experiments, the change in SAW amplitude occurred within the first few minutes of the chamber evacuation, when the pressure in the chamber dropped from atmospheric to pressures on the order of 10^{-2} mbars. Further pumping to reach even lower pressures produced no discernible changes in amplitude, and the attenuation coefficient due to argon or air gas was therefore calculated by taking the average value of SAW amplitude in vacuum and gas.

To carry out the experiment with argon the chamber first had to be pumped down to remove the air, which was done for 1 h before the chamber was re-filled with argon up to atmospheric pressure. The connecting gas tubes were flushed with argon before each use to remove unwanted contaminants. The chamber was initially slightly over-pressurised and then allowed to reach atmospheric pressure to ensure consistency with the air experiments. The device was left to rest for 10 min in the argon before the vacuum pump was switched on again for fifty minutes, in an identical manner to the air experiments.

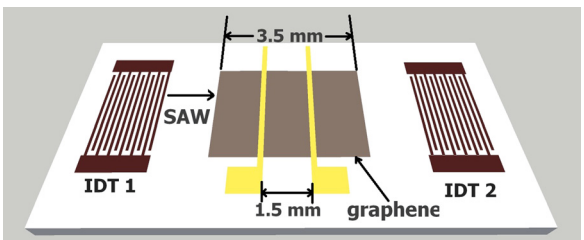

FIG. 2. Schematic diagram of the sample layout, showing transferred graphene region deposited on the quartz substrate.

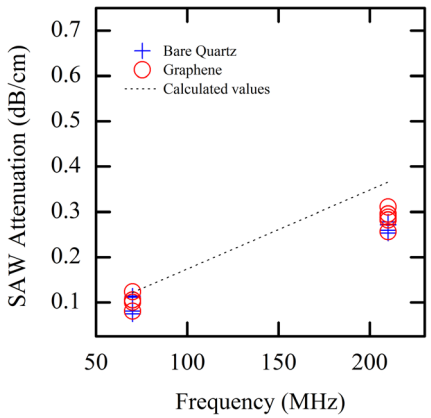

FIG. 3. Measured and calculated SAW attenuation at 70 MHz and 210 MHz for argon loading.

In Figure 3, measured values of attenuation coefficient due to argon loading, for both bare quartz devices and those containing graphene in the acoustic path, are shown for SAW frequencies of 70 MHz and 210 MHz. Each point represents a different measurement. As can be seen, there is no significant difference in the values of attenuation coefficient obtained for the graphene and non-graphene devices, with the average values attenuation coefficient for the bare quartz devices of 0.095 dB/cm and 0.266 dB/cm at 70 MHz and 210 MHz, respectively, compared to values of 0.103 dB/cm and 0.288 dB/cm obtained from the graphene devices. Also plotted in Figure 4 are values of attenuation coefficient calculated using the model developed by Slobodnik,[11]

$$\alpha = \frac{fP}{\rho_s v_s^2}\left(\frac{\gamma M}{RT}\right)^2, \tag{1}$$

where α is the attenuation (Nepers per metre), f is the SAW frequency, P is the pressure of the gas (Pascals), ρ_s is the density of the substrate (kilograms per cubic metre), ν_s is the velocity of the SAW in the substrate (metres per second), M is molecular mass of the gas, R is the universal gas constant, T is the temperature, and γ is the ratio of the specific heat at constant pressure to the specific heat at constant volume.[11] The values of attenuation calculated using Eq. (1) agree well with those measured, with both show increasing attenuation

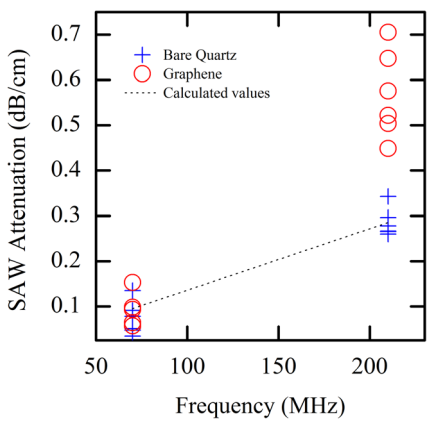

FIG. 4. Measured and calculated SAW attenuation at 70 MHz and 210 MHz for air loading.

with frequency (the calculated values are slightly higher than the attenuation measured experimentally at both frequencies, but this is expected from approximations in the theory and the difference between the measured and theoretical values of attenuation is of the same order and form as those measured by Slobodnik).[11]

In Figure 4, the attenuation due to air loading is shown for the bare quartz and graphene devices at 70 MHz and 210 MHz. At 70 MHz there is no significant difference between the graphene and non-graphene devices and the measured attenuation is consistent with the value of attenuation due to gas loading calculated from Eq. (1). However, at 210 MHz, there is a significant difference between the values of attenuation obtained from the graphene (average attenuation 0.57 dB/cm) and non-graphene devices (average attenuation 0.28 dB/cm), with the higher values of attenuation obtained from the graphene devices being not explained by just gas loading. Figure 5 shows the change in measured SAW amplitude on evacuation of the vacuum chamber for one of the graphene devices (the data chosen corresponding to the largest value of attenuation obtained). It is well known that water will be absorbed onto the surface of graphene,[12] will act to dope the graphene,[13] and can be trapped under CVD graphene when this is transferred to other substrates.[14] Water absorption could attenuate the SAW either through a viscoelastic mechanism,[2] or via the interaction of the electrostatic fields associated with the SAW travelling on a piezoelectric substrate and charge carriers within the graphene (acousto-electric attenuation). SAWs have been extensively used over the last decade to probe the magnetoconductivity of two-dimensional electron and hole systems.[15] The piezoelectric interaction between SAWs and 2D electrons is usually described using a simple classical relaxation model,[15] where the attenuation per unit length Γ is a non-monotonic function of the diagonal component of the conductivity tensor σ_{xx}^{2D},

$$\Gamma = q\frac{K_{eff}^2}{2}\left[\frac{(\sigma_{xx}^{2D}/\sigma_M)}{1+(\sigma_{xx}^{2D}/\sigma_M)^2}\right], \tag{2}$$

where q is the SAW wavevector, and K_{eff}^2 is the piezoelectric coupling coefficient. The maximum attenuation occurs at a characteristic conductivity σ_M is therefore given by

$$\Gamma_{Max} = q\frac{K_{eff}^2}{4}. \tag{3}$$

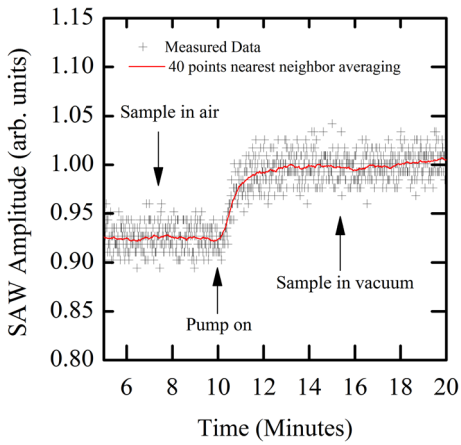

FIG. 5. Change in measured SAW amplitude on evacuation of the vacuum chamber for one of the graphene devices. The red line shows the raw data smoothed using nearest neighbor averaging with a 40 point window.

Taking values of 3158 m/s and 6×10^{-4} for the SAW velocity and K_{eff}^2 in ST quartz, the maximum attenuation predicted by this simple classical model would be approximately 2.7 dB/cm. As the chamber was evacuated, the resistance of the graphene devices was typically observed to decrease sharply by approximately 5% within the first few minutes, over similar timescales/pressures as the increase in attenuation. On further pumping, the resistance of the devices then started to increase slowly with time/decreasing pressure, so that after pumping for 20 h, reaching a pressure of $\sim 10^{-6}$ mbar, the resistance of the devices typically rises by around 10%, and continues to rise with further pumping. As a value of the characteristic conductivity, σ_M, or even the validity of the classical relaxation model, has yet to be established for graphene, it is not possible from these measurements alone to infer whether the change in the SAW amplitude on evacuation was due to the change in electrical characteristics of the graphene.

However, this sudden decrease in the device resistance on evacuation of the chamber is consistent with the removal of water vapour from the surface of the graphene.[16] In addition, the average change in attenuation observed for the graphene devices on evacuation of the chamber at 210 MHz (0.57 dB/cm) is similar to the value of the change in SAW attenuation ($\sim$0.55 dB/cm) obtained experimentally by Čiplys *et al.*[8] at a frequency of 286 MHz for relative humidity of 50% (which is the typical of the conditions in the laboratory in which the measurements presented here were undertaken). As the piezoelectric coupling coefficient of the Y-cut Z-propagation lithium niobate used by Čiplys *et al.* is approximately 40× greater than the quartz substrates used here, the similar values of the attenuation obtained in the two experiments suggest that the dominant attenuation mechanism is not acousto-electric, as any piezoelectric interaction with the charge carriers would scale linearly with the coupling coefficient and the attenuation would then be expected to be 40× larger when lithium niobate substrates are used. Instead, it is likely that the water absorbed onto the graphene causes attenuation via a viscoelastic effect. The relatively large variation in values of attenuation measured using the graphene devices is then likely to be due to variation in the starting condition of the device.

The attenuation of four SAW quartz devices was evaluated at two frequencies (70 MHz and 210 MHz) due to air and argon loading. Two of the devices had graphene transferred to their propagation path which produced an increase in attenuation with air loading compared to the non-graphene devices at 210 MHz which is not predicted by simple gas loading. Comparison to previous work using lithium niobate substrates suggests that this extra attenuation is due to the removal of water from the surface of the graphene and is visco-elastic rather than acousto-electric in nature. These measurements demonstrate the feasibility of the integration of graphene with SAW quartz devices.

The authors would like to thank Chris Bumstead, Stavroula Foteinopoulou, David Horsell, Alan Usher, and Charles Williams for useful discussions, and acknowledge the financial support of the Royal Society (Grant no.RG100570).

[1]Y. Dan, Y. Lu, N. J. Kybert, Z. Luo, and A. T. C. Johnson, Nano Lett. **9**, 1472 (2009).
[2]D. S. Ballantine, R. M. White, S. J. Martin, A. J. Ricco, E. T. Zellers, G. C. Frye, and H. Wohltjen, *Acoustic Wave Sensors: Theory, Design, and Physico-Chemical Applications* (Academic Press, San Diego, 1997).
[3]P. Thalmeier, B. Dora, and K. Ziegler, Phys. Rev. B **81**, 041409(R) (2010).
[4]S. H. Zhang and W. Xu, AIP Adv. **1**, 022146 (2011).
[5]V. Miseikis, J. E. Cunningham, K. Saeed, R. O'Rorke, and A. G. Davies, Appl. Phys. Lett. **100**, 133105 (2012).
[6]P. V. Santos, T. Schumann, M. H. Oliveira, J. M. J. Lopes, and H. Riechert, Appl. Phys. Lett. **102**, 221907 (2013).
[7]R. R. Arsat, M. Breedon, M. Shafiei, P. G. Spizziri, S. Gilje, R. B. Kaner, K. Kalantarzadeh, and W. Wlodarski, Chem. Phys. Lett. **467**, 344 (2009).
[8]D. Čiplys, R. Rimeika, A. Sereika, V. Poderys, R. Rotomskis, and M. S. Shur, Proceedings of the Ninth IEEE Sensors Conference, Hawaii, IEEE Pub. No. CFP10SEN-PRT (IEEE, New York, 2010), pp. 787–788.
[9]X. Li, W. Cai, J. An, S. Kim, J. Nah, D. Yang, R. Piner, A. Velamakanni, I. Jung, E. Tutuc, S. K. Banerjee, L. Colombo, and R. S. Ruoff, Science **324**, 1312 (2009).
[10]A. C. Ferrari, J. C. Meyer, V. Scardaci, C. Casiraghi, M. Lazzeri, F. Mauri, S. Piscanec, D. Jiang, K. S. Novoselov, S. Roth, and A. K. Geim, Phys. Rev. Lett. **97**, 187401 (2006).
[11]A. J. Slobodnik, J. Appl. Phys. **43**, 2565 (1972).
[12]F. Schedin, A. K. Geim, S. V. Morozov, E. W. Hill, P. Blake, and M. I. Katsnelson, Nature Mater. **6**, 652 (2007).
[13]T. O. Wehling, A. I. Lichtenstein, and M. I. Katsnelson, Appl. Phys. Lett. **93**, 202110 (2008).
[14]J. Chan, A. Venugopal, A. Pirkle, S. McDonnell, D. Hinojos, C. W. Magnuson, R. S. Ruoff, L. Colombo, R. M. Wallace, and E. M. Vogel, ACS Nano **6**, 3224 (2012).
[15]A. Wixforth, J. Scriba, M. Wassermeier, J. P. Kotthaus, G. Weimann, and W. Schlapp, Phys. Rev. B **40**, 7874 (1989).
[16]A. A. Kaverzin, A. S. Mayorov, A. Shytov, and D. W. Horsell, Phys. Rev. B. **85**, 075435 (2012).